



1 **Effects of Secondary Organic Aerosol Water on fine**
2 **PM levels and composition over US**

3
4
5 Stylianos Kakavas^{1,2}, Spyros N. Pandis^{1,2} and Athanasios Nenes^{1,3}

6 ¹Institute of Chemical Engineering Sciences, Foundation for Research and
7 Technology Hellas, Patras, Greece

8 ²Department of Chemical Engineering, University of Patras, Patras, Greece

9 ³School of Architecture, Civil and Environmental Engineering, École Polytechnique
10 Fédérale de Lausanne (EPFL), Switzerland

11

12 *Correspondence to:* Spyros N. Pandis (spyros@chemeng.upatras.gr) and Athanasios
13 Nenes (athanasios.nenes@epfl.ch).

14

15 **Abstract.** Water is a key component of atmospheric aerosol, affecting many aerosol
16 processes including gas/particle partitioning of semi-volatile compounds. Water
17 related to secondary organic aerosol (SOAW) is often neglected in atmospheric
18 chemical transport models and is not considered in gas-to-particle partitioning
19 calculations for inorganic species. We use a new inorganic aerosol thermodynamics
20 model, ISORROPIA-lite, which considers the effects of SOAW, to perform chemical
21 transport model simulations for a year over the continental United States to quantify
22 its effects on aerosol mass concentration and composition. SOAW can increase
23 average fine aerosol water levels up to a factor of two when secondary organic aerosol
24 (SOA) is a major PM₁ component. This is often the case in the south-eastern U.S
25 where SOA concentrations are higher. Although the annual average impact of this
26 added water on total dry PM₁ concentrations due to increased partitioning of nitrate
27 and ammonium is small (up to 0.1 μg m⁻³), total dry PM₁ increases of up to 2 μg m⁻³
28 (with nitrate levels increases up to 200%) can occur when RH levels and PM₁
29 concentrations are high.

30

31 **1. Introduction**

32 Fine atmospheric particulate matter with aerodynamic diameter smaller than 2.5 μm
33 (PM_{2.5}) has adverse effects on public health, climate and ecosystem productivity (Pye
34 et al., 2020; Baker et al., 2021; Guo et al., 2021). PM_{2.5} is composed of thousands of
35 organic compounds, black carbon (BC), and inorganic components such as sulfate



36 (SO₄²⁻), nitrate (NO₃⁻), ammonium (NH₄⁺) and chloride (Cl⁻) (Seinfeld and Pandis,
37 2006). Potassium (K⁺) levels can also be significant during biomass burning events
38 (Zhang et al., 2015; Pye et al., 2020). Ambient aerosol is mostly composed of water
39 which is determined by the chemical equilibrium of water vapor with the aerosol
40 constituents (Liao and Seinfeld, 2005; Carlton and Turpin, 2013; Guo et al., 2015;
41 Bougiatioti et al., 2016; Nguyen et al., 2016; Guo et al., 2017; Song et al., 2018; Pye
42 et al., 2020).

43 The hygroscopicity parameter (κ), which expresses the ability of a PM
44 component to absorb water, is an effective approach for the parameterization of the
45 water uptake of atmospheric PM that is a mixture of organic and inorganic species
46 (Petters and Kreidenweis, 2007). Although organic aerosol (OA) is less hygroscopic
47 than inorganic salts, it can still contribute significantly to the total aerosol water (Guo
48 et al., 2015; Bougiatioti et al., 2016; Jathar et al., 2016) or can even become the
49 dominant contributor at lower ambient relative humidity (Jin et al., 2020). Previous
50 studies have demonstrated that secondary organic aerosol (SOA) is a lot more
51 hygroscopic than primary organic aerosol (POA) and is mainly responsible for the
52 corresponding OA water (Koehler et al., 2009; Jathar et al., 2016).

53 SOAW can enhance secondary inorganic aerosol concentrations assisting in
54 their partitioning in the particulate phase to satisfy equilibrium. However, such effects
55 are not considered in thermodynamic modules used for the simulation of gas-to-
56 particle partitioning of inorganic species in chemical transport models. Evidence
57 exists however that fine aerosol nitrate and ammonium concentrations can increase in
58 areas with high organic aerosol and RH levels (Kakavas et al., 2022). The importance
59 of these SOAW impacts on secondary aerosol formation has not been systematically
60 studied and is the focus of this work.

61 We use a new aerosol thermodynamics model, ISORROPIA-lite (Kakavas et
62 al., 2022), to simulate SOAW effects on the partitioning of the inorganic components,
63 for a year over the continental United States. The model performance has been
64 evaluated for fine PM and its components for the examined period by Skyllakou et al.
65 (2021). The aim of our work is to quantify the SOAW contribution to the total fine
66 PM water and to study its effects on inorganic aerosol thermodynamics and total dry
67 fine PM levels and composition.

68

69 2. Methods



70 **2.1 ISORROPIA-lite**

71 ISORROPIA-lite is a lean and accelerated version of the widely used ISORROPIA-II
72 (Fountoukis and Nenes, 2007) aerosol thermodynamics model. It assumes that the
73 aerosol exists only in the metastable state at low RH and the activity coefficients of
74 ionic pairs are always obtained from precalculated look-up tables. It estimates aerosol
75 water associated with each one of the aerosol components. Furthermore,
76 ISORROPIA-lite has an important additional feature compared to ISORROPIA-II, as
77 it considers the effects of SOAW on inorganic aerosol thermodynamics. The resulting
78 increase of the total water mass drives more of the water-soluble gaseous species to
79 the particle phase to satisfy equilibrium. SOAW, W_{SOA} , in ISORROPIA-lite is
80 calculated using the well-established κ -Kohler theory of Petters and Kreidenweis
81 (2007):

$$82 \quad W_{SOA} = \frac{\rho_w}{\rho_{SOA}} \frac{C_{SOA} \kappa}{\left(\frac{1}{RH} - 1\right)} \quad (1)$$

83 where ρ_w is the density of water, ρ_{SOA} the SOA density, C_{SOA} the SOA concentration, κ
84 the SOA hygroscopicity parameter and RH the relative humidity in the 0–1 scale.
85 More details about the ISORROPIA-lite can be found in Kakavas et al. (2022).

86

87 **2.2 PMCAMx description and application**

88 PMCAMx (Karydis et al., 2010; Tsimpidi et al., 2010) is a three dimensional
89 chemical transport model based on CAMx (Environ, 2006), which simulates
90 horizontal and vertical advection and dispersion, dry and wet deposition, as well as
91 aqueous, gas, and aerosol chemistry. The mechanism used in this work for gas-phase
92 chemistry simulations is the Carbon Bond 05 (CB5) (Yarwood et al., 2005) and
93 includes 190 reactions of 79 gas species. To describe the aerosol size and composition
94 distribution 10-size sections (from 40 nm to 40 μm) are used assuming that all
95 particles in each size bin have the same composition. Equilibrium is always assumed
96 between the bulk aerosol and gas phases. The partitioning of semi-volatile inorganic
97 species between the gas and particulate phases is simulated by ISORROPIA-lite.
98 Weighting factors based on each size bin's effective surface area are used to distribute
99 to the various size bins the mass transferred between the two phases in each time step
100 (Pandis et al., 1993). For the simulation of organic aerosols, the volatility basis set
101 approach (Donahue et al., 2006) is used. POA is simulated using eight volatility bins



102 (from 10^{-1} to $10^6 \mu\text{g m}^{-3}$) at 298 K, while for SOA four volatility bins (1 , 10 , 10^2 ,
103 $10^3 \mu\text{g m}^{-3}$) at 298 K are used (Murphy and Pandis, 2009). For the major point
104 sources, the NO_x plumes are simulated using the Plume-in-Grid (PiG) approach
105 (Karamchandani et al., 2011; Zakoura and Pandis, 2019).

106 We applied PMCAMx over the continental United States during 2010. The
107 modeling domain includes northern Mexico and southern Canada and covers a $4752 \times$
108 2952 km^2 region (Figure S1). The model grid consists of 10,824 cells with horizontal
109 dimensions of $36 \times 36 \text{ km}$. The meteorological inputs were provided by the Weather
110 Research Forecasting model (WRF v3.6.1) using a horizontal resolution of $12 \times$
111 12 km . The gaseous and primary particle emissions were developed by Xing et
112 al. (2013). More details about the meteorological inputs and the emissions can be
113 found in Skyllakou et al. (2021).

114 To quantify the SOAW effects on inorganic aerosol thermodynamics three
115 simulations were performed. The first was a simulation neglecting SOAW and
116 including only inorganic aerosol water. Two additional simulations were performed:
117 one where κ of SOA was assumed to be equal to 0.1 and one with $\kappa=0.2$ to examine
118 how SOA hygroscopicity affects total fine aerosol water content and PM levels and
119 composition. A SOA density of 1 g cm^{-3} was assumed in the simulations. The SOA
120 exists mostly in submicrometer particles so our subsequent study focuses on PM_{10} .

121

122 3. Results

123 3.1 Effects of SOAW on PM_{10} water levels

124 The annual average PM_{10} water ground-level concentrations neglecting SOAW are
125 shown in Figure 1. Higher PM_{10} water concentrations from 8 to $18 \mu\text{g m}^{-3}$ are
126 predicted in the north-eastern part of the US due to the higher inorganic PM_{10}
127 concentrations (Figure S2) and RH levels in that area. When SOAW is present in the
128 simulations, total PM_{10} water levels increase everywhere with higher fractional
129 increases in the south-eastern US (up to 50% when $\kappa=0.1$ and up to 100% when $\kappa=0.2$
130 in Alabama and north-western Mexico) due to higher SOA levels (Figure S3). In the
131 north-eastern US, lower fractional increases are predicted (10–15% when $\kappa=0.1$ and
132 20–30% when $\kappa=0.2$). In general, assuming a κ of SOA equal to 0.2 instead of 0.1
133 increases the corresponding amount of SOAW by about a factor of two. Figure 1
134 shows the distributions of fractional increase change in the annual PM_{10} water levels at
135 ground level from SOAW. Total PM_{10} water average concentrations increase from 20



136 to 30% in about 60% of the modeling domain when $\kappa=0.1$. For $\kappa=0.2$, the
137 corresponding increase is from 40 to 60%.

138 Predicted SOA levels are higher during summertime (Figure S3) since the
139 emissions and oxidation rates of volatile organic compounds (VOCs) are higher
140 (Zhang et al., 2013; Freney et al., 2014; Skyllakou et al., 2014; Fountoukis et al.,
141 2016). However, even during wintertime fresh biomass burning emissions exposed to
142 NO_2 and O_3 can form significant amounts of SOA in periods with low OH levels
143 (Kodros et al., 2020). Higher total PM_{10} water concentrations are predicted during
144 winter (Figure S4) since the RH levels and inorganic fine aerosol concentrations are
145 higher; especially nitrate and chloride which increasingly partition to the aerosol
146 phase as temperature decreases (Guo et al., 2017). Higher fractional increases in fine
147 aerosol water levels (up to 5 times) due to SOAW are predicted during summer in the
148 south-eastern part of US where SOA concentrations are higher. This corresponds to
149 increases to average fine aerosol water concentrations up to $8 \mu\text{g m}^{-3}$.

150 Ammonium nitrate and ammonium sulfate are the inorganic salts that
151 contribute the most to the total PM_{10} water levels (Figure S5). SOAW also contributes
152 significantly to the total PM_{10} water levels especially in the south-eastern US (about 30
153 and 50% of total PM_{10} water when $\kappa=0.1$ and $\kappa=0.2$ respectively), when the mass
154 fraction of SOA in dry PM_{10} exceeds 30%.

155

156 3.2 Effects of SOAW on total dry PM_{10} levels

157 Higher dry PM_{10} concentrations are predicted for the eastern part of the US (up to 15
158 $\mu\text{g m}^{-3}$) in the base case (Figure 2). These dry PM_{10} levels increase slightly up to 0.6%
159 and 1.2% due to SOAW when $\kappa=0.1$ and $\kappa=0.2$ for SOA is assumed. The highest
160 annual average fractional increase in total dry PM_{10} levels is predicted in California
161 (1% when $\kappa=0.1$ and 2% when $\kappa=0.2$). The probability density (Figure 2) indicates
162 that in about 60% of the modeling domain total dry fine aerosol concentrations
163 increase up to 0.3% when $\kappa=0.1$. For $\kappa=0.2$, the corresponding increase is from 0.4 to
164 2%. The areas of the highest PM_{10} increase correspond to regions where aerosol pH
165 tends to be relatively high (Pye et al., 2020). In these areas, nitric acid and ammonia
166 can condense and increase aerosol mass because of the increase in water from the
167 SOA. Because of this partitioning change, the predicted gas-phase concentrations of
168 semi-volatile inorganic components decreased on average when SOAW was
169 considered (Figure S6). SOAW had a negligible absolute impact on the small fine



170 chloride concentrations in this period (Figure S2). However, in periods during which
171 chloride salts and SOA contribute significantly to the total dry (e.g. during intense
172 biomass burning periods), fine chloride concentrations could also change (Metzger et
173 al., 2006; Fountoukis et al., 2009; Gunthe et al., 2021).

174

175 **3.3 Effects of SOAW on PM₁ components**

176 The annual average results indicate that SOAW mainly affects fine aerosol water
177 levels. To better analyze the effects of SOAW we focus on the temporal evolution of
178 the predicted levels of PM₁ components in four sites (Figure S1) with different
179 characteristics (Table S1). The presence of SOAW increased PM₁ water
180 concentrations in all sites from 1% to almost an order of magnitude (Figure 3).
181 However, these fractional increases most of the time correspond to PM₁ water
182 concentration increases of a few $\mu\text{g m}^{-3}$ (Figure S7) because they occur under low RH
183 levels. During higher RH periods (80 to 100%), the PM₁ water levels are predicted to
184 increase up to $100 \mu\text{g m}^{-3}$ (e.g. in Toronto).

185 Total dry PM₁ concentrations during most of the simulated period increase on
186 average less than 1% in all sites (Figure 3) due to SOAW. There are periods, however,
187 with higher fractional increases (up to 10%) and even small decreases (up to 5%) in
188 total dry fine aerosol levels in the examined sites. The decreases can be explained
189 because SOAW increases the size of particles and therefore their dry deposition rate
190 (Nenes et al., 2020). Depending on SOA hygroscopicity, increases up to $1.5 \mu\text{g m}^{-3}$
191 for nitrate and $0.5 \mu\text{g m}^{-3}$ for ammonium are predicted (Figure S7). Fine nitrate
192 increases of 10% were more frequent in the examined sites; however higher increases
193 up to 200% are predicted during the simulated period (Figure 4). As expected, higher
194 increases can occur more often with higher assumed SOA hygroscopicity.

195

196 **4. Discussion**

197 Aerosol liquid water has a profound impact on aerosol processes, chemical
198 composition and their impacts. By including the effects of organic water on
199 inorganics thermodynamic equilibrium we show that SOAW can substantially
200 increase aerosol water levels, on an average up to 60% over the majority of the
201 domain. As a consequence, total dry PM₁ levels can also increase but the changes are
202 small (up to 2% on an annual average basis). Locally these effects can be much more



203 significant during periods of high RH and SOA levels (fine nitrate fractional increases
204 can be as high as 200%).

205 The effects vary with season. During summer, the RH is lower and SOA levels
206 are higher leading to higher fractional increases in aerosol water (Figure S4) but lower
207 absolute mass changes. During summer the fractional increases in total dry fine
208 aerosol concentrations are lower than in wintertime (Figure S8). Responsible for the
209 total dry fine aerosol concentration increases are nitrate and ammonium (Figure S2).
210 These compounds partition together (as deliquesced ammonium nitrate) to the
211 particulate phase to satisfy equilibrium due to the additional water mass of SOA.

212 The increases in total dry PM₁ and fine aerosol water levels depend on SOA
213 concentrations, hygroscopicity value, RH levels and the particle phase fractions of
214 inorganic species. The SOAW effect on aerosol water is approximately proportional
215 to the assumed hygroscopicity parameter κ .

216 Aerosol liquid water directly affects the PM sensitivity and dry deposition
217 rates, with direct implications for emissions control policy (Nenes et al., 2020; Nenes
218 et al., 2021; Sun et al., 2021). Given this, and the important role of SOAW for climate
219 forcing, visibility and chemistry, its inclusion in future studies is highly
220 recommended. ISORROPIA-lite provides a simple and computationally effective
221 approach for the simulation of SOAW.

222

223 **Code and Data Availability.** The model code and data used in this study are available
224 from the authors upon request (spyros@chemeng.upatras.gr and
225 athanasios.nenes@epfl.ch).

226

227 **Author Contributions.** SK incorporated ISORROPIA-lite in PMCAMx, carried out the
228 simulations, analyzed the results and wrote the manuscript. SN and AN conceived and
229 led the study and helped in the writing of the manuscript.

230

231 **Competing Interests.** The authors declare no competing financial interest.

232

233 **Acknowledgements.** This work was supported by the project FORCeS funded from
234 the European Union's Horizon 2020 research and innovation programme under grant
235 agreement No 821205, and project PyroTRACH (ERC-2016-COG) funded from



236 H2020-EU.1.1. - Excellent Science - European Research Council (ERC), project ID
237 726165.

238

239 **References**

240 Baker, A., Kanakidou, M., Nenes, A., Myriokefalitakis, S., Croot, P.L., Duce, A. D.,
241 Gao, Y., Guieu, C., Ito, A., Jickells, T. D., Mahowald, N. M., Middag, R.,
242 Perron, M. M. G., Sarin, M. M., Shelley, R., and Turner, D. R.: Changing
243 atmospheric acidity as a modulator of nutrient deposition and ocean
244 biogeochemistry, *Sci. Adv.*, 7, doi: 10.1126/sciadv.abd8800, 2021.

245 Bougiatioti, A., Nikolaou, P., Stavroulas, I., Kouvarakis, G., Weber, R., Nenes, A.,
246 Kanakidou, M., and Mihalopoulos, N.: Particle water and pH in the eastern
247 Mediterranean: source variability and implications for nutrient availability,
248 *Atmos. Chem. Phys.*, 16, 4579–4591, 2016.

249 Carlton, A. G. and Turpin, B. J.: Particle partitioning potential of organic compounds
250 is highest in the Eastern US and driven by anthropogenic water, *Atmos. Chem.*
251 *Phys.*, 13, 10203–10214, 2013.

252 Donahue, N. M., Robinson, A. L., Stanier, C. O., and Pandis, S. N.: Coupled
253 partitioning, dilution, and chemical aging of semivolatile organics, *Environ.*
254 *Sci. Technol.*, 40, 2635–2643, 2006.

255 Environ: Comprehensive Air Quality Model with Extensions Version 4.40. Users
256 Guide. ENVIRON Int. Corp., Novato, CA, <http://www.camx.com>, 2006.

257 Fountoukis, C. and Nenes, A.: ISORROPIA II: a computationally efficient
258 thermodynamic equilibrium model for K^+ - Ca^{2+} - Mg^{2+} - NH_4^+ - Na^+ - SO_4^{2-} - NO_3^- -
259 Cl^- - H_2O aerosols, *Atmos. Chem. Phys.*, 7, 4639–4659, 2007.

260 Fountoukis, C., Nenes, A., Sullivan, A., Weber, R., Van Reken, T., Fischer, M.,
261 Matías, E., Moya, M., Farmer, D., and Cohen, R. C.: Thermodynamic
262 characterization of Mexico City aerosol during MILAGRO 2006, *Atmos.*
263 *Chem. Phys.*, 9, 2141–2156, 2009.

264 Fountoukis, C., Megaritis, A. G., Skyllakou, K., Charalampidis, P. E.,
265 Denier van der Gon, H. A. C., Crippa, M., Prévôt, A. S. H., Fachinger, F.,
266 Wiedensohler, A., Pilinis, C., and Pandis, S. N.: Simulating the formation of
267 carbonaceous aerosol in a European Megacity (Paris) during the MEGAPOLI
268 summer and winter campaigns, *Atmos. Chem. Phys.*, 16, 3727–3741, 2016.



- 269 Freney, E. J., Sellegri, K., Canonaco, F., Colomb, A., Borbon, A., Michoud, V.,
270 Doussin, J.-F., Crumeyrolle, S., Amarouche, N., Pichon, J.-M., Bourianne, T.,
271 Gomes, L., Prevot, A. S. H., Beekmann, M., and Schwarzenböck, A.:
272 Characterizing the impact of urban emissions on regional aerosol particles:
273 airborne measurements during the MEGAPOLI experiment, *Atmos. Chem.*
274 *Phys.*, 14, 1397–1412, 2014.
- 275 Gunthe, S. S., Liu, P., Panda, U., Raj, S. S., Sharma, A., Derbyshire, E., Reyes-
276 Villegas E., Allan, J., Chen, Y., Wang, X., Song, S., Pöhlker, M. L., Shi, L.,
277 Wang, Y., Kommula, S. M., Liu, T., Ravikrishna, R., McFiggans, G., Mickey,
278 L. J., Martin, S. T., Pöschl, U., Andreae, M. O., and Coe, H.: Enhanced
279 aerosol particle growth sustained by high continental chlorine emission in
280 India., *Nat. Geosci.*, 14, 77–84, 2021.
- 281 Guo, H., Xu, L., Bougiatioti, A., Cerully, K. M., Capps, S. L., Hite Jr., J. R., Carlton,
282 A. G., Lee, S.-H., Bergin, M. H., Ng, N. L., Nenes, A., and Weber, R. J.: Fine-
283 particle water and pH in the southeastern United States, *Atmos. Chem. Phys.*
284 15, 5211–5228, 2015.
- 285 Guo, H., Liu, J., Froyd, K. D., Roberts, J. M., Veres, P. R., Hayes, P. L., Jimenez, J.
286 L., Nenes, A., and Weber, R. J.: Fine particle pH and gas–particle phase
287 partitioning of inorganic species in Pasadena, California, during the 2010
288 CalNex campaign, *Atmos. Chem. Phys.*, 17, 5703–5719, 2017.
- 289 Guo, H., Li, X., Li, W., Wu, J., Wang, S., and Wei, J.: Climatic modification effects
290 on the association between PM₁ and lung cancer incidence in China, *BMC*
291 *public health*, 21, 880, 2021.
- 292 Jathar, S.H., Mahmud, A., Barsanti, K.C., Asher, W. E., Pankow, J. F., and Kleeman
293 M. J.: Water uptake by organic aerosol and its influence on gas/particle
294 partitioning of secondary organic aerosol in the United States, *Atmos.*
295 *Environ.*, 129, 142–154, 2016.
- 296 Jin, X., Wang, Y., Li, Z., Zhang, F., Xu, W., Sun, Y., Fan, X., Chen, G., Wu, H., Ren,
297 J., Wang, Q., and Cribb, M.: Significant contribution of organics to aerosol
298 liquid water content in winter in Beijing, China, *Atmos. Chem. Phys.*, 20,
299 901–914, 2020.
- 300 Kakavas, S., Pandis, S. N., and Nenes, A.: ISORROPIA-lite: A comprehensive
301 atmospheric aerosol thermodynamics module for Earth System Models, *Tellus*
302 *B*, 74, 1–23, 2022.



- 303 Karamchandani, P., Vijayaraghavan, K., and Yarwood, G.: Sub-grid scale plume
304 modeling, *Atmosphere*, 2, 389–406, 2011.
- 305 Karydis, V. A., Tsimpidi, A. P., Fountoukis, C., Nenes, A., Zavala, M., Lei, W.,
306 Molina, L. T., and Pandis, S. N.: Simulating the fine and coarse inorganic
307 particulate matter concentrations in a polluted megacity, *Atmos. Environ.*, 44,
308 608–620, 2010.
- 309 Kodros, J. K., Papanastasiou, D. K., Paglione, M., Masiol, M., Squizzato, S., Florou,
310 K., Skyllakou, K., Kaltsonoudis, C., Nenes, A., and Pandis, S. N.: Rapid Dark
311 Aging of Biomass Burning as an Overlooked Source of Oxidized Organic
312 Aerosol., *Proc. Natl. Acad. Sci. U.S.A.*, 117, 33028–33033, 2020.
- 313 Koehler, K. A., Kreidenweis, S. M., DeMott, P. J., Petters, M. D., Prenni, A. J., and
314 Carrico, C. M.: Hygroscopicity and cloud droplet activation of mineral dust
315 aerosol, *Geoph. Res. Let.*, 36, (8), 2009.
- 316 Liao, H. and Seinfeld, J. H.: Global impacts of gas-phase chemistry aerosol
317 interactions on direct radiative forcing by anthropogenic aerosols and ozone, *J.*
318 *Geophys. Res.*, 110, D18208, 2005.
- 319 Metzger, S., Mihalopoulos, N., and Lelieveld, J.: Importance of mineral cations and
320 organics in gas-aerosol partitioning of reactive nitrogen compounds: case
321 study based on MINOS results., *Atmos. Chem. Phys.*, 6, 2549–2567, 2006.
- 322 Murphy, B. N. and Pandis, S. N.: Exploring summertime organic aerosol formation in
323 the Eastern United States using a regional-scale budget approach and ambient
324 measurements, *J. Geophys. Res.*, 115, (D24216), 2010.
- 325 Nenes, A., Pandis, S. N., Weber, R. J., and Russell, A.: Aerosol pH and liquid water
326 content determine when particulate matter is sensitive to ammonia and nitrate
327 availability, *Atmos. Chem. Phys.*, 20, 3249–3258, 2020.
- 328 Nenes, A., Pandis, S. N., Kanakidou, M., Russell, A. G., Song, S., Vasilakos, P., and
329 Weber, R. J.: Aerosol acidity and liquid water content regulate the dry
330 deposition of inorganic reactive nitrogen, *Atmos. Chem. Phys.*, 21, 6023–
331 6033, 2021.
- 332 Nguyen, T. K. V., Zhang, Q., Jimenez, J. L., Pike, M., and Carlton, A. G.: Liquid
333 water: ubiquitous contributor to aerosol mass. *Environ. Sci. Tech. Let.*, 3,
334 257–263, 2016.



- 335 Pandis, S. N., Wexler, A. S., and Seinfeld, J. H.: Secondary organic aerosol formation
336 and transport – II. Predicting the ambient secondary organic aerosol size
337 distribution, *Atmos. Environ.*, 27, 2403–2416, 1993.
- 338 Petters, M. D. and Kreidenweis, S. M.: A single parameter representation of
339 hygroscopic growth and cloud condensation nucleus activity, *Atmos. Chem.*
340 *Phys.*, 7, 1961–1971, 2007.
- 341 Pye, H. O. T., Nenes, A., Alexander, B., Ault, A. P., Barth, M. C., Clegg, S. L.,
342 Collett Jr, J. L., Fahey, K. M., Hennigan, C. J., Herrmann, H., Kanakidou, M.,
343 Kelly, J. T., Ku, I.-T., McNeill, V. F., Riemer, N., Schaefer, T., Shi, G.,
344 Tilgner, A., Walker, J. T., Wang, T., Weber, R., Xing, J., Zaveri, R. A., and
345 Zuend, A.: The acidity of atmospheric particles and clouds, *Atmos. Chem.*
346 *Phys.*, 20, 4809–4888, 2020.
- 347 Seinfeld, J. H. and Pandis, S. N.: *Atmospheric chemistry and physics: From air*
348 *pollution to climate change*, Wiley: New York, 2006.
- 349 Skyllakou, K., Murphy, B. N., Megaritis, A. G., Fountoukis, C., and Pandis, S. N.:
350 Contributions of local and regional sources to fine PM in the megacity of
351 Paris, *Atmos. Chem. Phys.*, 14, 2343–2352, 2014.
- 352 Skyllakou, K., Rivera, P. G., Dinkelacker, B., Karnezi, E., Kioutsioukis, I.,
353 Hernandez, C., Adams, P. J., and Pandis, S. N.: Changes in
354 PM_{2.5} concentrations and their sources in the US from 1990 to 2010, *Atmos.*
355 *Chem. Phys.*, 21, 17115–17132, 2021.
- 356 Song, S., Gao, M., Xu, W., Shao, J., Shi, G., Wang, S., Wang, Y., Sun, Y., and
357 McElroy, M. B.: Fine-particle pH for Beijing winter haze as inferred from
358 different thermodynamic equilibrium models, *Atmos. Chem. Phys.*, 18, 7423–
359 7438, 2018.
- 360 Sun, X., Ivey, C. E., Baker, K. R., Nenes, A., Lareau, N. P., and Holmes, H. A.:
361 Confronting Uncertainties of Simulated Air Pollution Concentrations during
362 Persistent Cold Air Pool Events in the Salt Lake Valley, Utah., *Environ. Sci.*
363 *Technol.*, 55, 15072–15081, 2021.
- 364 Tsimpidi, A. P., Karydis, V. A., Zavala, M., Lei, W., Molina, L., Ulbrich, I. M.,
365 Jimenez, J. L., and Pandis, S. N.: Evaluation of the volatility basis-set
366 approach for the simulation of organic aerosol formation in the Mexico City
367 metropolitan area, *Atmos. Chem. Phys.*, 10, 525–546, 2010.



368 Xing, J., Pleim, J., Mathur, R., Pouliot, G., Hogrefe, C., Gan, C.-M., and Wei, C.:
369 Historical gaseous and primary aerosol emissions in the United States from
370 1990 to 2010, *Atmos. Chem. Phys.*, 13, 7531–7549, 2013.

371 Yarwood, G., Rao, S., Yocke, M., and Whitten, G. Z.: Updates to the Carbon Bond
372 Chemical Mechanism: CB05, Research Triangle Park, [https://camx-
373 wp.azurewebsites.net/Files/CB05_Final_Report_120805.pdf](https://camx-wp.azurewebsites.net/Files/CB05_Final_Report_120805.pdf), 2005.

374 Zakoura, M. and Pandis, S. N.: Improving fine aerosol nitrate predictions using a
375 Plume-in-Grid modeling approach, *Atmos. Environ.*, 215, 116887, 2019.

376 Zhang, Q. J., Beekmann, M., Drewnick, F., Freutel, F., Schneider, J., Crippa, M.,
377 Prevot, A. S. H., Baltensperger, U., Poulain, L., Wiedensohler, A., Sciare, J.,
378 Gros, V., Borbon, A., Colomb, A., Michoud, V., Doussin, J.-F., Denier van
379 der Gon, H. A. C., Haeffelin, M., Dupont, J.-C., Siour, G., Petetin, H.,
380 Bessagnet, B., Pandis, S. N., Hodzic, A., Sanchez, O., Honoré, C., and
381 Perrussel, O.: Formation of organic aerosol in the Paris region during the
382 MEGAPOLI summer campaign: evaluation of the volatility basis-set approach
383 within the CHIMERE model, *Atmos. Chem. Phys.*, 13, 5767–5790, 2013.

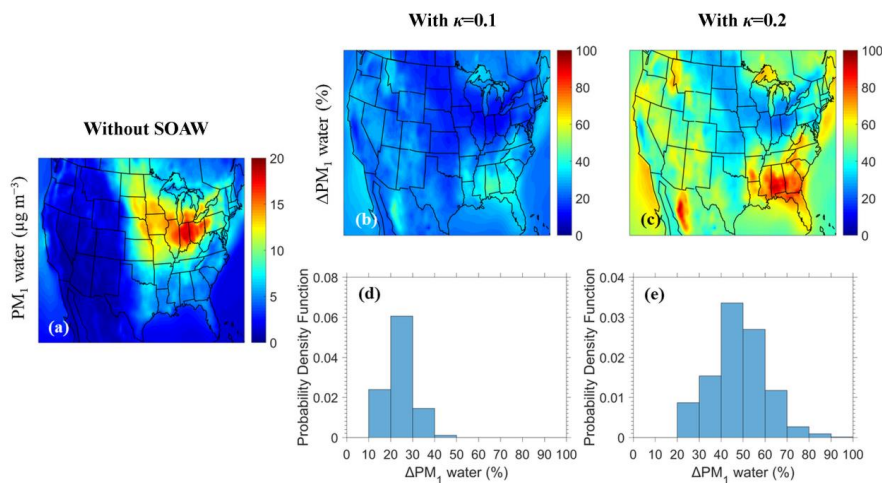
384 Zhang, Z., Gao, J., Engling, G., Tao, J., Chai, F., Zhang, L., Zhang, R., Sang, X.,
385 Chan, C., Lin, Z., and Cao, J.: Characteristics and applications of size-
386 segregated biomass burning tracers in China’s Pearl River Delta region,
387 *Atmos. Environ.*, 102, 290–301, 2015.

388
389
390
391
392
393
394
395
396
397
398
399
400
401
402
403



404

405



406

407

408 **Figure 1.** Maps of: (a) annual average PM₁ water ground-level concentrations
409 neglecting SOAW, (b) annual average fractional increase of PM₁ water when SOAW
410 is present in the simulations with $\kappa=0.1$ and, (c) with $\kappa=0.2$ during 2010. The
411 probability density as a function of fractional increase in the annual PM₁ water
412 concentrations due to SOAW when: (d) $\kappa=0.1$ and (e) $\kappa=0.2$ is shown.

413

414

415

416

417

418

419

420

421

422

423

424

425

426

427

428

429

430

431

432

433

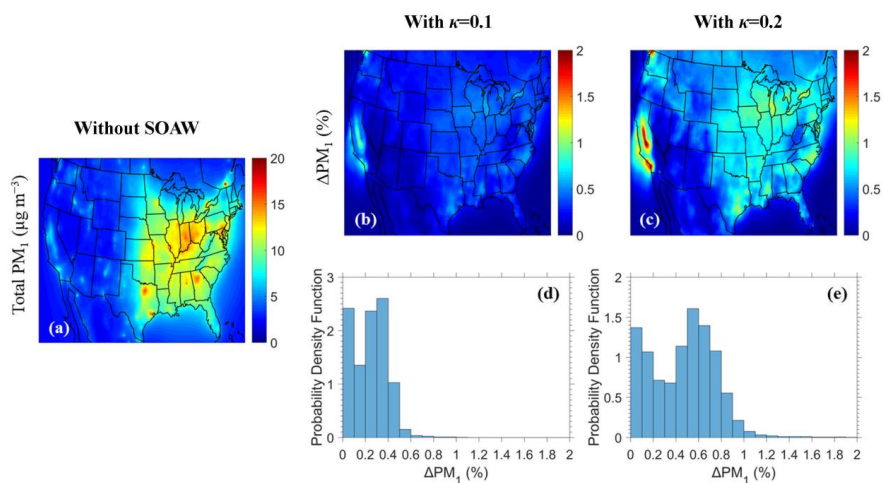
434

435



436

437



438

439

440 **Figure 2.** Maps of: (a) annual average total dry PM₁ ground-level concentrations
441 neglecting SOAW, (b) annual average fractional increase of total dry PM₁ when
442 SOAW is present in the simulations with $\kappa=0.1$ and, (c) with $\kappa=0.2$ during 2010. The
443 probability density as a function of fractional increase in the annual total dry PM₁
444 concentrations due to SOAW when: (d) $\kappa=0.1$ and (e) $\kappa=0.2$ is shown.

445

446

447

448

449

450

451

452

453

454

455

456

457

458

459

460

461

462

463

464

465

466

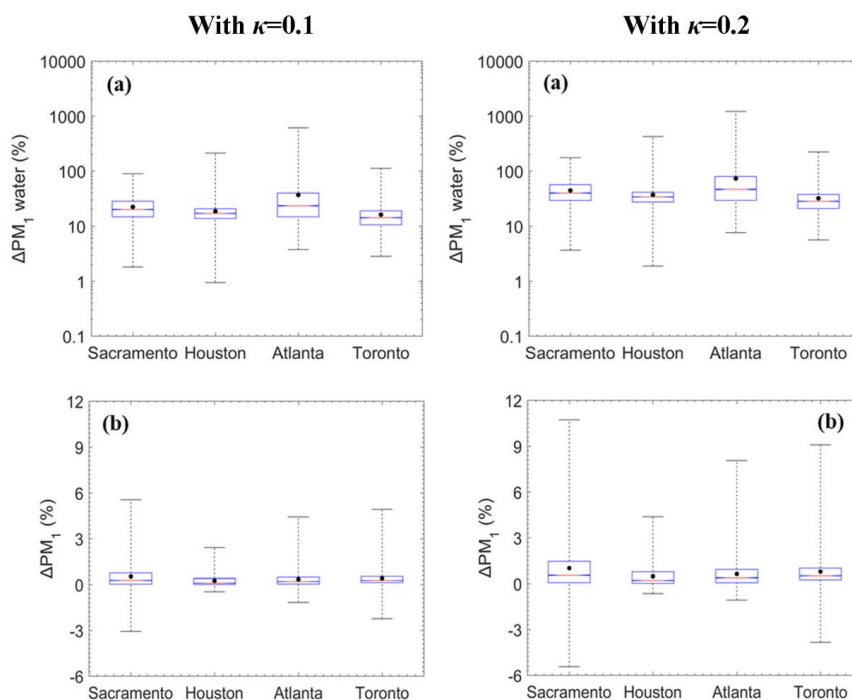
467

468



469

470



471

472

473 **Figure 3.** Box plots for fractional change in the hourly: (a) PM₁ water and (b) total
474 dry PM₁ due to SOAW when $\kappa=0.1$ and $\kappa=0.2$ for Sacramento, California; Houston,
475 Texas; Atlanta, Georgia; and Toronto, Canada during 2010. The red line represents
476 the median, the black dot is the mean value, the upper box line is the upper quartile
477 (75%) and the lower box line is the lower quartile (25%) of the distribution. A
478 negative change corresponds to a decrease.

479

480

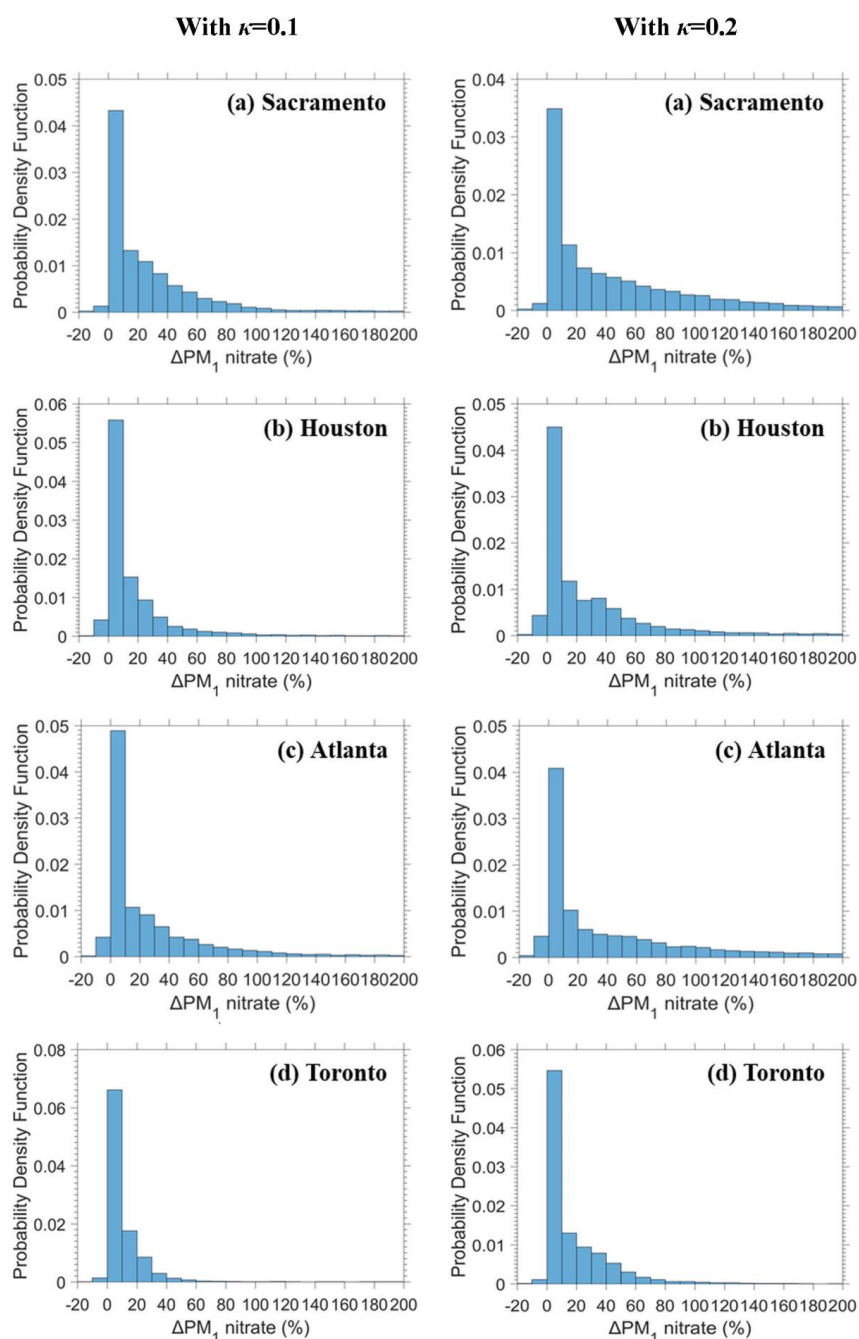
481

482

483

484

485



486

487

488 **Figure 4.** The probability density as a function of fractional increase in the hourly
489 PM_1 nitrate due to SOAW when $\kappa=0.1$ and $\kappa=0.2$ for: **(a)** Sacramento, California; **(b)**
490 Houston, Texas; **(c)** Atlanta, Georgia; and **(d)** Toronto, Canada during 2010.